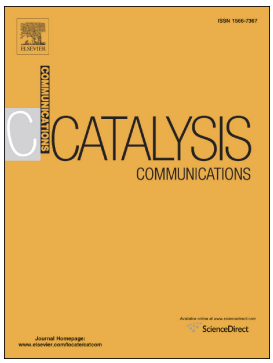

MFI vs. FER zeolite during methanol dehydration to dimethyl ether: The crystal size plays a key role

Enrico Catizzone, Alfredo Aloise, Emanuele Giglio, Giorgia Ferrarelli, Micaela Bianco, Massimo Migliori, Girolamo Giordano

PII: S1566-7367(20)30290-9

DOI: https://doi.org/10.1016/j.catcom.2020.106214

Reference: CATCOM 106214

To appear in: *Catalysis Communications*

Received date: 25 June 2020

Revised date: 22 October 2020

Accepted date: 28 October 2020

Please cite this article as: E. Catizzone, A. Aloise, E. Giglio, et al., MFI vs. FER zeolite during methanol dehydration to dimethyl ether: The crystal size plays a key role, *Catalysis Communications* (2020), https://doi.org/10.1016/j.catcom.2020.106214

MFI vs. FER zeolite during methanol dehydration to dimethyl ether: the crystal size plays a key role

In honor of Professor James G. Goodwin, Jr. on the occasion of his 75th birthday, to celebrate his outstanding contribution to heterogeneous catalysis, and his remarkable role in the knowledge diffusion in the field of catalysis science and technology as Editor-in-Chief of Catalysis Communication.

Enrico CATIZZONE[§,*], Alfredo ALOISE, Emanuele GIGLIO, Giorgia FERRARELLI, Micaela BIANCO[§§], Massimo MIGLIORI, Girolamo GIORDANO

Laboratory of Catalysis and Industrial Chemistry, University of Calabria, Via P. Bucci – I-87036 Rende, Italy.

[§]Present affiliation: ENEA, Italian National Agency for New Technologies, Energy and Sustainable Economic Development, Trisaia Research Centre, Rotondella, I-75026, Italy

[§§]Present affiliation: Waste to Methane S.r.l., Via M. Polo, Rende (CS) Italy

*Corresponding author

E-mail address: enrico.catizzone@enea.it

Phone: +39-0835-374319

ABSTRACT

FER-type zeolite was recently recognized as good catalyst for DME synthesis via methanol dehydration or one-pot CO_2 hydrogenation, in terms of DME selectivity, stability and coke formation. In this research, we investigated the role of crystal size of both FER- and MFI-type zeolites on catalysis of methanol dehydration to DME reaction. The results show that FER-type zeolites, both micro- and nano-sized, exhibit better performances than micro-sized MFI-type zeolite. On the contrary, the application of nano-sized MFI allows to obtain a DME selectivity similar to FER, but with higher DME production rate and a lower coke deposition.

Keywords: methanol conversion; dimethyl ether; molecular sieves; crystal size; nanosized zeolites; coke formation.

1. INTRODUCTION

The Dimethyl-ether (DME) synthesis via one-pot CO_2 hydrogenation, is an emerging strategy to propose DME as "green fuel" alternative to Diesel engines, also because of its high cetane number and eco-friendly emissions [1, 2]. DME can be then considered a reliable energy vector to introduce renewable energy in the chemical industry as it could recycle CO_2 (from biomasses or capture processes) in combination with renewable hydrogen. Currently, DME is commercialized as substitute to liquefied petroleum gas (LPG). Moreover, DME can also act as an intermediate in olefins production in methanol-to-olefins (MTO) process [3, 4].

DME is industrially-obtained via either the methanol dehydration (indirect route) or the one-pot syngas conversion (direct route) [5]. In the indirect route, methanol (MeOH) is synthesized by CO hydrogenation over Cu/ZnO-based catalysts and then dehydrated to DME over an acid catalyst in a separate reactor. In the direct route both the synthesis and the subsequent dehydration of methanol are carried out in a single reactor over a redox/acid multifunctional catalyst under process conditions close to those of the methanol synthesis (240–280°C, 3–7 MPa). Details, perspectives and challenges about innovative one-pot CO_2 hydrogenation process are discussed elsewhere [6-8]. Whatever the synthesis route, the physicochemical properties of the acid catalyst for the methanol dehydration reaction step play a key role in DME production rate and catalyst stability.

Traditionally, γ-Al_2O_3 plays the role of acid catalyst for the either the dehydration of methanol to dimethyl ether (indirect route) or as co-catalyst, coupled with redox catalyst (e.g. Cu/ZnO/Al_2O_3), for the direct route converting syngas [9, 10]. γ-Al_2O_3 exhibits very low DME productivity during CO_2-to-DME process, due to low resistance in presence of the large amount of water produced during the reaction. Therefore, due to their higher resistance in presence of water, zeolites acid catalysts are largely investigated both in one-pot CO_2-to-DME process and in vapour phase methanol dehydration [11-15].

Due to their very regular networks of channels and cages with well-defined sized and shapes, zeolites are largely used in several industrial applications (heterogeneous catalysis, gas separation, ion exchange) [16, 17]. Both advantages and disadvantages are related to the regular micropore channel system. Among the advantages, shape selectivity is the most important aspect when zeolites are used in either catalysis or separation, while the main drawback is the severe mass transport limitations inside the

crystals, especially when zeolites are applied in catalysis. During the past decades, much effort was devoted to prepare zeolites with enhanced diffusion inside the crystal [18, 19] and the synthesis of nanosized zeolite crystals was largely investigated as a promising strategy to prepare a material with reduced mass transfer limitations [20, 21].

Recent works showed that the zeolite structure (channels opening and orientation) strongly affects catalyst behaviour during methanol dehydration, mainly in terms of deactivation and coke deposition. Among the several zeolite structures investigated until now, FER-type zeolite (2-dimensional 8/10-membered rings channel system) seems to exhibit the best performances in terms of DME selectivity and coke-induced deactivation [22-25]. In a recent study, the positive effect of crystal size reduction of FER-type zeolite on DME productivity and coke deposition was reported [26]. Compared to other investigated zeolite structure (MTW, EUO, TON, beta, MOR, CHA), studies on MFI-type zeolite showed that this structure exhibits a good stability but with lower DME productivity and higher coke formation, due to larger pore structure than that of FER-type zeolite [27, 28]. As mentioned before, the properties of zeolites strongly depend on the synthesis conditions. In this study, we highlight that zeolite crystal size plays a crucial role and, therefore, performances comparison of different structures could be a relative concept, when this parameter is not properly addressed. Zeolites may be considered as a chemical reactor at nanometric scale: the control of residence time inside the crystal/reactor is of paramount importance, especially to inhibit consecutive reactions, such as in the case of MeOH/DME-to-hydrocarbons reactions. In this work, both micro- and nano-sized zeolites with MFI or FER structure are compared, with the aim to show how the control of diffusional phenomena may be more important than shape-selectivity.

2. EXPERIMENTAL

Micro-sized FER sample (M-FER) was synthesised with pyrrolidine as structure directing agent (SDA) by adopting the following gel molar composition:

$$0.6\ \text{Pyrrolidine} - 0.08\ Na_2O - 0.05\ Al_2O_3 - 1\ SiO_2 - 20\ H_2O$$

For the synthesis 1.69 g of sodium aluminate and 0.17 g of NaOH were dissolved in 39.8 g of distilled water. 6.3 g of pyrrolidine were then added and the solution was mixed for 30 minutes. Afterwards, 22 g of colloidal silica were added dropwise. After 1 h of aging under vigorous stirring (500 rpm) the obtained gel was crystallised in a 90 ml PTFE-lined stainless steel autoclave using a tumbling oven (tumbling speed = 20 rpm) kept at 180 °C for 120 h.

Nano-sized FER sample (N-FER) was synthesised by using seeds prepared by adopting the same condition of M-FER but with the addition of sodium lauryl sulphate (SLS) with a SLS/Al_2O_3 molar ratio equals to 0.3. The same gel composition of M-FER was adopted for N-FER but with the addition of 3 wt % of seeds (calculated on silica basis). The obtained gel was aged at 80 °C for 48 h under stirring (500 rpm) and the crystallised at 160 °C for 60 h.

Micro-sized MFI-type sample (M-MFI) was prepared by using tetrapropyl ammonium bromide (TPABr) as SDA, starting from a gel with the following molar composition:

$$0.10\ Na_2O - 0.08\ \text{TPABr} - 0.02\ Al_2O_3 - 1\ SiO_2 - 20\ H2O$$

Briefly 2.66 g of NaOH, 1.04 g of $Al(OH)_3$ and 7.1 g of TPABr were dissolved in 119.3 g of distilled water. 20 g of precipitated silica was then added and the resulting gel was stirred for 1 h at room temperature before being transferred in a PTFE-lined stainless steel autoclave and kept in a static oven at 175 °C for 120 h for crystallization.

A gel with the same molar composition of M-MFI sample was aged for 96 h at 30 °C and then heated at 170 °C for 96 h to obtain nano-sized MFI-type sample (N-MFI).

After crystallisation, the solids were recovered by filtration, washed several times with distilled water, and dried at 105 °C for 8 h. In order to remove organics from the structure, the samples were calcined in air flow at 550 °C for 8. The acidic form was obtained after two cycles (2 h each at 80 °C) of ion exchange with NH_4Cl 1 M solution, followed by calcination in air flow at 550 °C for 8 h.

The crystalline structure of samples was analysed by X-ray powder diffraction (APD 2000 Pro, GNR analytic instrument, Italy) in the range 5°-50° 2theta range. Crystals morphology was observed by scanning electronic microscopy (FEI model Inspect). The Si/Al ratio in the solid was measured by atomic absorption spectroscopy (GBC 932). Textural properties (e.g. BET surface area, pore volume) were determined by adsorption/desorption isotherms of N_2 at 77 K (ASAP2020, Micromeritics). Total acidity was estimated by ammonia titration by following a procedure discussed elsewhere [29]. Catalytic tests were performed in an experimental apparatus equipped with a tubular reactor described elsewhere [30], by adopting the following conditions: methanol/N_2 (molar ratio 0.056/0.944) as feed mixture, WHSV = 4 $g \cdot g_{cat}^{-1} \cdot h^{-1}$, temperature =120-240 °C, atmospheric pressure. After 20 h Time-on-stream tests at 240 °C, used catalysts were recovered and carbon deposit was analysed by

thermogravimetric analysis and GC-MS technique, with a procedure detailed elsewhere [25].

3. RESULTS AND DISCUSSION

3.1 Characterization

Figure 1 reports the XRD patterns of the investigated zeolites which show high crystallinity with no impurities.

HERE FIGURE 1

The SEM images of the investigated zeolites are reported in **Figure 2**. The crystals of M-FER sample exhibit a typical plate like shape with a well-defined [1 0 0] face with length around 10 µm, length/width ratio around 2 and thickness around 100 nm [31]. N-FER sample consists of smaller crystallites with a size around 100 nm. M-MFI sample exhibit a prismatic-like crystal shape with a size of about 3x6 µm, typical of Al-containing MFI zeolites [32]. The SEM image of N-MFI sample clearly shoes the beneficial effect of aging on crystal size reduction. In fact, N-MFI samples consists of crystals with size around 300 nm. Larger crystals up to 1 µm are also formed.

HERE FIGURE 2

NH_3-TPD profiles of the investigated zeolites are reported in **Figure 3**. All the samples exhibit a similar NH_3 evolution profile, with two main desorption bands in the temperature range 150-300 °C and 300-600 °C, which indicate the presence of two

different families of acid sites, namely weak and strong, respectively. For FER-type zeolites a band at temperatures higher than 700 °C is also present, which may be associated to dehydroxylation phenomena, as demonstrated elsewhere [33].

HERE FIGURE 3

A summary of the acidic and other physicochemical properties of the investigated samples is reported in **Table 1**.

HERE TABLE 1

Bulk chemical analysis shows the Si/Al molar ratio in the solid is very similar to that adopted during the preparation of synthesis gel. FER-type zeolites exhibit a higher acidity than MFI-type zeolites due to the higher aluminium content. Surface area and micropore volume are very similar of microporous FER- or MFI-type zeolites.

3.2 Catalytic tests

The catalytic activity during methanol dehydration was investigated in the temperature range 120-240 °C and the measured methanol conversion is reported in Figure 4. The thermodynamics equilibrium conversion for methanol dehydration to DME is also reported.

HERE FIGURE 4

For all the investigated catalysts, higher methanol conversion occurred with increasing reaction temperature. N-FER sample exhibited the highest methanol conversion in the investigated temperature range. Similar performance was observed for M-FER and N-MFI, while M-MFI shows the lowest activity. A DME selectivity equals to 1 was measured for all the samples in temperature range 120-220 °C.

At 240 °C, C1-C3 hydrocarbons were detected in the products stream for M-FER, M-MFI and N-MFI which shows a DME selectivity around 0.96. In order to better clarify the effect of crystals dimensions, DME selectivity was also measured at 280 °C. At this temperature, DME selectivity was 0.86 over M-FER, 0.98 over N-FER, 0.75 over M-MFI and 0.94 over N-MFI. These results clearly show that the decrease of residence time inside the crystals, induced by the crystal size lowering, reduces the formation of by-products, such as light hydrocarbons. In particular, the total C1-C3 hydrocarbons yield was about 7% (on carbon basis) for M-MFI sample, and 1.7% for N-MFI sample. Data at 280 °C clearly showed the crystal size effect, but this high temperature is not suitable for DME synthesis, especially for the one-pot CO_2 hydrogenation, as the formation of CO by reverse water gas shift and the sintering of metal catalyst particles can significantly affect the overall process performances [8].

In order to assess the acid sites efficiency of investigated samples, DME production rate was calculated by taking into account the acid sites concentration measured by NH_3-TPD technique, in the reaction temperature-range 180-240 °C.

As reported in secondary axis of **Figure 4**, although the values calculated at 240 °C may be affected by thermodynamics constrain, N-MFI sample exhibits the highest DME production rate in the investigated temperature range. By comparing samples with the same zeolite framework, reaction rate increases as the crystal size decreases, due to the

reduction of mass transfer limitations which lead to an improvement of the catalytic crystal efficiency. Therefore, it may be concluded that crystal size reduction strongly enhances both the accessibility to acid sites and diffusion rate. As a consequence, DME formation rate can be improved accordingly. It is also noteworthy that acidity of M-MFI and N-MFI is below 5% (**Table 1**) and catalytic test are carried out under the same WHSV, therefore the observed improvement on activity and productivity on N-MFI samples could be directly attributed to the reduced size of the crystal. The same consideration cannot be directly done for FER samples as the difference in acidity of N-FER and M-FER is above 30%, therefore different test conditions were adopted to analyse the effect of crystal size for these samples. Data reported in Appendix A confirmed, also for FER-type, the positive effect of nanosizing the crystal in terms of catalyst performances.

The apparent activation energy values were calculated by Arrhenius plot of the conversion data obtained in the temperature range 120-160 °C (see Appendix A). The obtained values are 78 kJ/mol for M-FER, 46 kJ/mol for N-FER, 97 kJ/mol for M-MFI and 73 kJ/mol for N-MFI. The results indicate that apparent activation energy decreases with crystal size, which may be a consequence of the lowering of activation energy, related to configurational/activated diffusion.

The catalysts effectiveness factor (η) has been evaluated also in a simplified form, to elucidate the role of intra-particle mass diffusion limitation according to a literature procedure [34] and details about calculation are reported in Appendix A. Whatever the structure adopted, data indicates that catalyst effectiveness approaches the unity for nanosized catalysts due to the reduction in transfer limitation. On the contrary, micro-sized samples exhibited an effectiveness lower of about one order of magnitude,

indicating the presence of a significant resistance to diffusion over the tested temperature interval, mainly due to the larger crystal size.

Catalyst stability was studied by time-on-stream tests at 240 °C for 20 h. As reported in **Table 2**, all the investigated catalysts exhibit a high stability in terms of methanol conversion.

HERE TABLE 2

N-FER sample is confirmed as the most selective catalyst with a DME selectivity stable at 0.99. N-MFI and M-FER shows similar DME selectivity, while a slight reduction in DME selectivity for M-MFI sample observed over time.

After time-on-stream tests, the reactor was purged with nitrogen and the used catalyst was then recovered and analysed to obtain insights about coke deposition. In **Table 2** the amount of coke deposited measured by TGA of used catalyst after 20 h time-on-stream is reported. Micro-sized samples exhibit a tendency to form coke significantly higher than nano-sized samples. During methanol dehydration reaction, coke is formed by oligomerization and cyclization reactions from light olefins to alkyl aromatics, both routes catalysed by strong acid sites. The superiority of nanosized zeolites may be reasonably related to the enhanced diffusional rate of both reactants and intermediates that retard the formation of coke. On the whole, N-MFI sample shows the lower amount of carbon deposit after time-on-stream. However, a deeper investigation about the location of coke would be useful to fully understand the role of crystal size on coke formation and deposition. From extraction procedure of deposited coke, no insoluble

coke was observed, suggesting that all the carbonaceous deposit can be referred as "soluble coke" [35].

The GC-MS spectra of extracted coke are reported in **Figure 5.**

HERE FIGURE 5

The analysis of mass spectra indicates the presence of poly substituted alkyl aromatics in all the investigated samples. In particular, coke consists mainly of tetra-methyl benzene for FER-type zeolites, while penta- and hexa-methyl benzene molecules were also found over MFI-type zeolites. In particular, hexa methyl benzene seems to be the most abundant specie over M-MFI, while tetra-methyl benzene is the most abundant specie over N-MFI. Such differences, which should be confirmed for longer period of reaction, may be also related to the crystal size. However, the formation of penta- and hexa-methyl benzene seems to be specific of MFI-type framework.

4. CONCLUSIONS

FER- and MFI-type zeolites are recognised as stable catalysts for DME synthesis. In this work, the role of crystal size of these zeolites on catalysis of methanol dehydration to DME reaction in the temperature range 180-240 °C was studied. The obtained results indicate that crystal size plays a crucial role in terms of DME production rate, DME selectivity and coke deposition. Nano-sized crystals exhibit superior performances than micro-sized crystals. In particular, nano-sized MFI shows a similar DME selectivity (>0.96) and conversion of micro-sized FER, but with a higher DME production rate and

a lower coke deposition. On the other hand, nano-sized FER shows the highest DME selectivity (>0.99). On the whole, zeolites may be considered as nano-scale reactor: by controlling the residence time is possible to have a control on products distribution in the case of consecutive reactions. Furthermore, the enhancing of diffusion rate by reduction of crystal size improves the efficiency of acid sites.

REFERENCES

[1] T.A. Semelsberger, R. L. Borup, H. L. Greene, Dimethyl ether (DME) as an alternative fuel, J. Power Source 156 (2006) 497-511. https://doi.org/10.1016/j.jpowsour.2005.05.082

[2] S.H. Park, C.S. Lee, Applicability of dimethyl ether (DME) in a compression ignition engine as an alternative fuel, Energy Convers. Manage. 86 (2014) 848-863. https://doi.org/10.1016/j.enconman.2014.06.051.

[3] S. Xu, Y. Zhi, J. Han, W. Zhang, X. Wu, T. Sun, Y. Wei, Z. Liu, Chapter Two - Advances in Catalysis for Methanol-to-Olefins Conversion, Adv. Catal. 61 (2017) 37-122. https://doi.org/10.1016/bs.acat.2017.10.002.

[4] P. Pérez-Uriarte, A. Ateka, T. Aguayo, A. G. Gayubo, J. Bilbao, Kinetic model for the reaction of DME to olefins over a HZSM-5 zeolite catalyst, Chem. Eng. J. 302 (2016) 801-810. https://doi.org/10.1016/j.cej.2016.05.096.

[5] Z. Azizi, M. Rezaeimanesh, T. Tohidian, M. R. Rahimpour, Dimethyl ether: A review of technologies and production challenges, Chem. Eng. Process. Proc. Intens. 82 (2014) 150-172. https://doi.org/10.1016/j.cep.2014.06.007.

[6] A. Álvarez, A. Bansode, A. Urakawa, A. V. Bavykina, T. A. Wezendonk, M. Makkee, J. Gascon, F. Kapteijn, Challenges in the Greener Production of Formates/Formic Acid, Methanol, and DME by Heterogeneously Catalyzed CO_2 Hydrogenation Processes, Chem. Rev. 117 (2017) 9804-9838. https://doi.org/10.1021/acs.chemrev.6b00816

[7] S. Perathoner, G. Centi, CO2 recycling: a key strategy to introduce green energy in the chemical production chain. ChemSusChem 7 (2014) 1274-1282. https://doi.org/10.1002/cssc.201300926.

[8] E. Catizzone, G. Bonura, M. Migliori, F. Frusteri, G. Giordano, CO_2 recycling to dimethyl ether: state-of-the-art and perspectives. Molecules 23 (2018) 31. https://doi.org/10.3390/molecules23010031.

[9] F. Raoof, M. Taghizadeh, A. Eliassi, F. Yaripour, Effects of temperature and feed composition on catalytic dehydration of methanol to dimethyl ether over γ-alumina, Fuel 87 (2008) 2967-2971. https://doi.org/10.1016/j.fuel.2008.03.025.

[10] H. Ham, J. Kim, S. J. Cho, J.-H. Choi, D. J. Moon, J. W. Bae, Enhanced Stability of Spatially Confined Copper Nanoparticles in an Ordered Mesoporous Alumina for Dimethyl Ether Synthesis from Syngas. ACS Catal. 6 (2016) 5629-5640. https://doi.org/10.1021/acscatal.6b00882.

[11] J. Boon, J. van Kampen, R. Hoogendoorn, S. Tanese, F. P. F. van Berkel, M. S. Annaland, Reversible deactivation of γ-alumina by steam in the gas-phase dehydration of methanol to dimethyl ether, Catal. Comm. 119 (2019) 22-27. https://doi.org/10.1016/j.catcom.2018.10.008.

[12] G. Bonura, C. Cannilla, L. Frusteri, E. Catizzone, S. Todaro, M. Migliori, G. Giordano, F. Frusteri, Interaction effects between CuO-ZnO-ZrO2 methanol phase and zeolite surface affecting stability of hybrid systems during one-step CO2 hydrogenation to DME, Catal. Today 345 (2020) 175-182. https://doi.org/10.1016/j.cattod.2019.08.014.

[13] F. Frusteri, M. Migliori, C. Cannilla, L. Frusteri, E. Catizzone, A. Aloise, G. Giordano, Direct CO2-to-DME hydrogenation reaction: New evidences of a superior behaviour of FER-based hybrid systems to obtain high DME yield, J. CO2 Util. 18 (2017) 353-361. http://dx.doi.org/10.1016/j.jcou.2017.01.030.

[14] F. Frusteri, M. Cordaro, C. Cannilla, G. Bonura, Multifunctionality of Cu–ZnO–ZrO2/H-ZSM5 catalysts for the one-step CO2-to-DME hydrogenation reaction, Appl. Catal. B: Env. 162 (2015) 57-65. https://doi.org/10.1016/j.apcatb.2014.06.035.

[15] E. Catizzone, M. Migliori, A. Purita, G. Giordano, Ferrierite vs. γ-Al_2O_3: The superiority of zeolites in terms of water-resistance in vapour-phase dehydration of methanol to dimethyl ether. J. Energy Chem. 30 (2019) 162-169. https://doi.org/10.1016/j.jechem.2018.05.004.

[16] A. Corma, A. Martinez, Zeolites and zeotypes as catalysts, Adv. Mater. 7 (1995) 134-144. https://doi.org/10.1002/adma.19950070206.

[17] M. Dusselier, M. E. Davis, Small-Pore Zeolites: Synthesis and Catalysis, Chem. Rev. 118 (2018) 5265-5329. . https://doi.org/10.1021/acs.chemrev.7b00738.

[18] F. Di Renzo, Zeolites as tailor-made catalysts: Control of the crystal size Catal. Today 41 (1998) 37-40. https://doi.org/10.1016/S0920-5861(98)00036-4.

[19] J. Čejka, G. Centi, J. Perez-Pariente, W. J. Roth, Zeolite-based materials for novel catalytic applications: Opportunities, perspectives and open problems. Catal. Today 179 (2012) 2-15.

[20] S. Mintova, M. Jaber, V. Valtchev, Nanosized microporous crystals: emerging applications, Chem. Soc. Rev. 44 (2015) 7207-7233. https://doi.org/10.1039/C5CS00210A.

[21] S. Mintova, J.-P. Gilson, V. Valtchev, Advances in nanosized zeolites, Nanoscale 5 (2013) 6693-6703. https://doi.org/10.1039/C3NR01629C.

[22] P.S.S. Prasad, J. W. Bae, S.-H. Kang, Y.-J. Lee, K.-W. Jun, Single-step synthesis of DME from syngas on Cu–ZnO–Al2O3/zeolite bifunctional catalysts: The superiority of ferrierite over the other zeolites, Fuel Process. Technol. 89 (2008) 1281-1286.

[23] R. Montesano, A. Narvaez, D. Chadwick, Shape-selectivity effects in syngas-to-dimethyl ether conversion over Cu/ZnO/Al2O3 and zeolite mixtures: Carbon deposition and by-product formation, Appl. Catal. A: Gen. 482 (2014) 69-77. https://doi.org/10.1016/j.apcata.2014.05.009.

[24] E. Catizzone, A. Aloise, M. Migliori, G. Giordano, Dimethyl ether synthesis via methanol dehydration: Effect of zeolite structure, Appl. Catal. A: Gen. 502 (2015) 215-220. https://doi.org/10.1016/j.apcata.2015.06.017.

[25] M. Migliori, E. Catizzone, A. Aloise, G. Bonura, L. Gómez-Hortigüela, L. Frusteri, C. Cannilla, F. Frusteri, G. Giordano, New insights about coke deposition in methanol-to-DME reaction over MOR-, MFI- and FER-type zeolites, J. Ind. Eng. Chem. 68 (2018) 196-208. https://doi.org/10.1016/j.jiec.2018.07.046.

[26] E. Catizzone, S. Van Daele, M. Bianco, A. Di Michele, A. Aloise, M. Migliori, V. Valtchev, G. Giordano, Catalytic application of ferrierite nanocrystals in vapour-phase dehydration of methanol to dimethyl ether, Appl. Catal. B: Env. 243 (2019) 273-282. https://doi.org/10.1016/j.apcatb.2018.10.060.

[27] G. Laugel, X. Nitsch, F. Ocampo, B. Louis, Methanol dehydration into dimethyl ether over ZSM-5 type zeolites: Raise in the operational temperature range, Appl. Catal. A: Gen. 402 (2011) 139-145. https://doi.org/10.1016/j.apcata.2011.05.039.

[28] E. Catizzone, A. Aloise, M. Migliori, G. Giordano, From 1-D to 3-D zeolite structures: performance assessment in catalysis of vapour-phase methanol dehydration to DME, Microp. Mesop. Mater. 243 (2017) 102-111. https://doi.org/10.1016/j.micromeso.2017.02.022.

[29] E. Catizzone, Z. Cirelli, A. Aloise, P. Lanzafame, M. Migliori, G. Giordano, Methanol conversion over ZSM-12, ZSM-22 and EU-1 zeolites: from DME to hydrocarbons production. Catal. Today 304 (2018) 39-50. http://dx.doi.org/10.1016/j.cattod.2017.08.037.

[30] M. Migliori, A. Aloise, E. Catizzone, G. Giordano, Kinetic analysis of methanol to dimethyl ether reaction over H-MFI catalyst, Ind. Eng. Chem. Res. 53 (2014) 14885-14891. http //dx.doi.org/10.1021/ie502775u.

[31] X. Chen, T. Todorova, A. Vimont, V. Ruaux, Z. Qin, J.-P. Gilson, V. Valtchev, In situ and post-synthesis control of physicochemical properties of FER-type crystals, Microp. Mesop. Mater. 200 (2014) 334-342. https://doi.org/10.1016/j.micromeso.2014.07.057.

[32] T. Armaroli, L. J. Simon, M. Digne, T. Montanari, M. Bevilacqua, V. Valtchev, J. Petarin, G. Busca, Effects of crystal size and Si/Al ratio on the surface properties of H-ZSM-5 zeolites, Appl. Catal. A: Gen. 306 (2006) 78-84. https://doi.org/10.1016/j.apcata.2006.03.030.

[33] E. Catizzone, M. Migliori, T. Mineva, S. van Daele, V. Valtchev, G. Giordano, New synthesis routes and catalytic applications of ferrierite crystals. Part 1: 1,8-Diaminooctane as a new OSDA, Microp. Mesop. Mater. 296 (2020) 109987. https://doi.org/10.1016/j.micromeso.2019.109987.

[34] J. Liang, Y. Mi, G. Song, H. Peng, Y. Li, R. Yan, W. Liu, Z. Wang, P. Wu, F. Liu, Environmental benign synthesis of Nano-SSZ-13 via FAU trans-crystallization: Enhanced NH3-SCR performance on Cu-SSZ-13 with nano-size effect, J. Hazard. Mater. 398 (2020) 122986. https://doi.org/10.1016/j.jhazmat.2020.122986.

[35] M. Guisnet, P. Magnoux, Organic chemistry of coke formation, Appl. Catal. A: Gen. 212, 2001, 83-96. https://doi.org/10.1016/S0926-860X(00)00845-0.

TABLES CAPTIONS

Table 1 – Summary of physicochemical properties of the investigated zeolites

Table 2 – Methanol conversion, DME selectivity and carbon deposit during time-on-stream tests. WHSV: 4 h^{-1}, Temperature: 240 °C.

FIGURES CAPTIONS

Figure 1 – XRD patterns of investigated zeolites

Figure 2 – SEM images of the investigated zeolites

Figure 3 – NH_3-TPD profiles of the investigated zeolites

Figure 4 – Methanol conversion (closed symbols) and DME production rate (open symbols) as a function of reaction temperature, WHSV: 4 h^{-1}.

Figure 5 – GC-MS spectra of carbon deposit extracted from soluble coke of studied samples after 20 h reaction at 240 °C, WHSV: 4 h^{-1}. MB: methyl benzene.

SAMPLE	Average crystal size (μm)	Si/Al[a] (mol/mol)	Acidity (μmol/g)		S_{BET}[c] (m^2/g)	V_{mic}[d] (cm^3/g)
			Weak[b]	Strong[b]		
M-FER	5x10	11	526	761	332	0.13
N-FER	0.1	11	274	523	304	0.12
M-MFI	3x6	27	218	343	386	0.13
N-MFI	0.3	23	281	300	371	0.12

[a] Determined by atomic absorption.

[b] From NH_3-TPD profiles: weak determined from ammonia desorption in the range 100-300 °C, strong determined from ammonia desorption above 300 °C, excluding dehydroxilation band.

[c] BET specific surface area

[d] Micropore volume calculated by t-plot method

Table 1

SAMPLE	*Methanol Conversion [-]*		*DME Selectivity [-]*		*Carbon deposit*
	after 15 min	*after 1200 min*	*after 15 min*	*after 1200 min*	*[mg/g]*
M-FER	0.81	0.81	0.96	0.96	61
N-FER	0.85	0.84	0.99	0.99	41
M-MFI	0.82	0.79	0.95	0.92	58
N-MFI	0.81	0.80	0.96	0.9(	36

Table 2

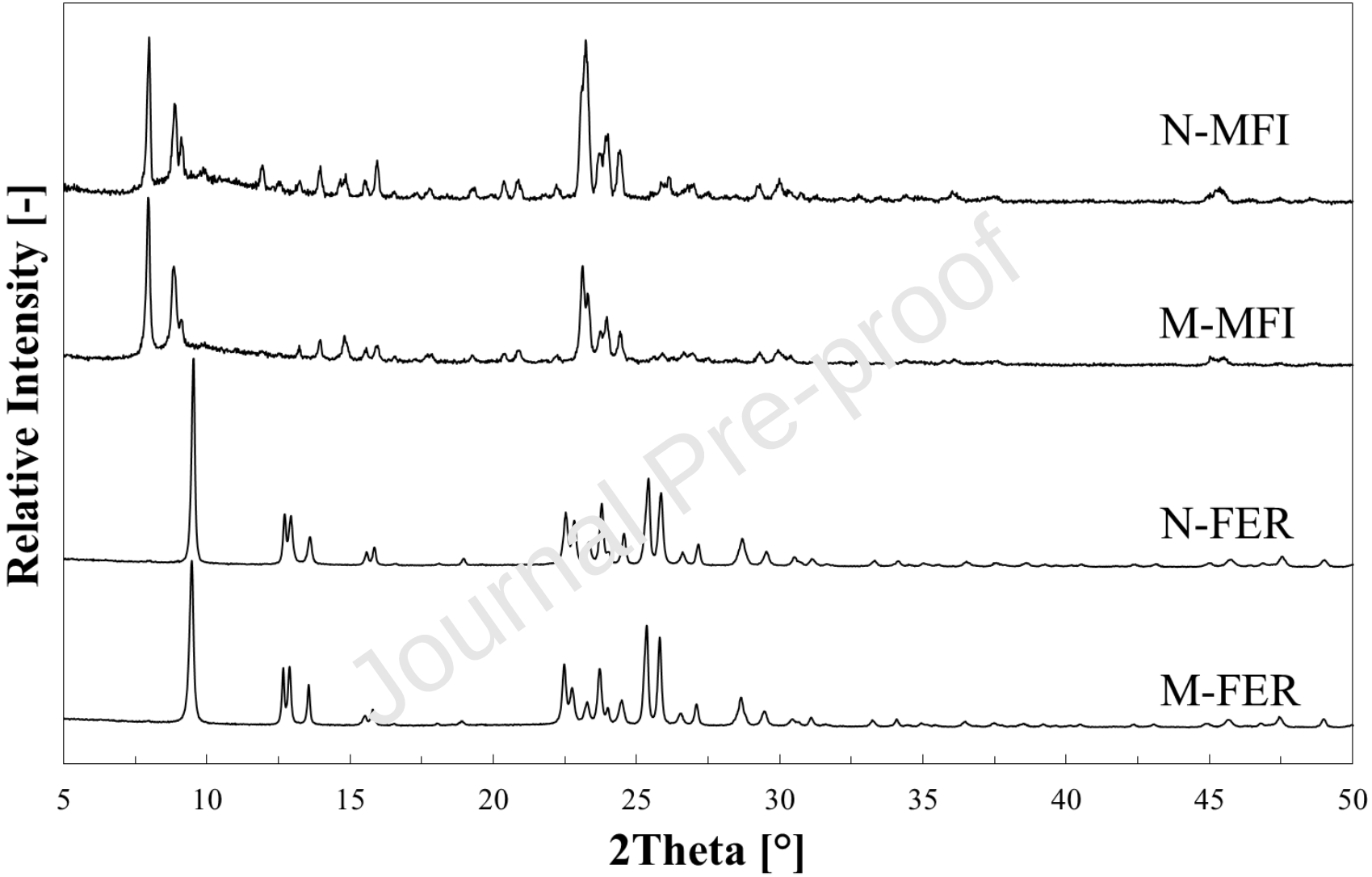

Figure 1

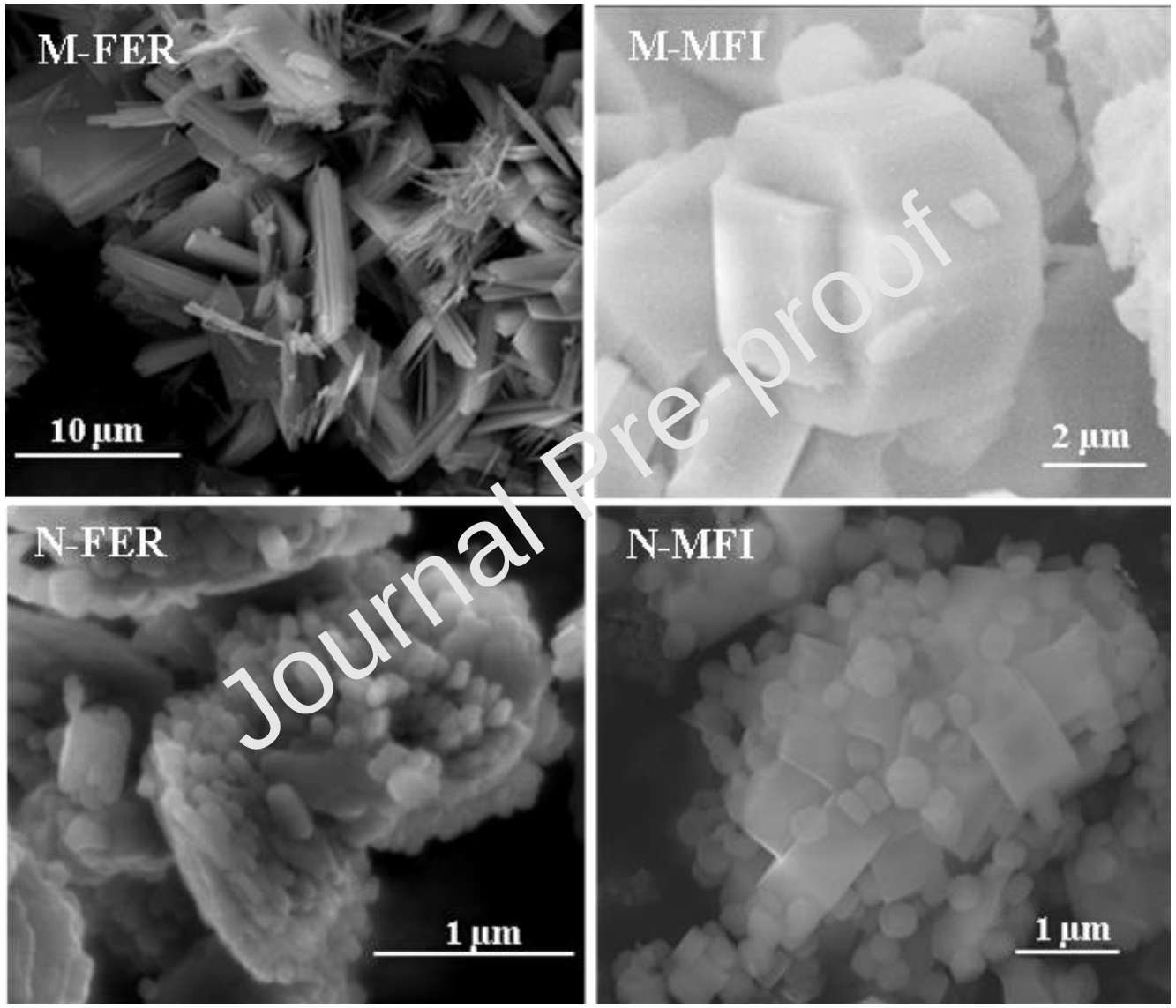

Figure 2

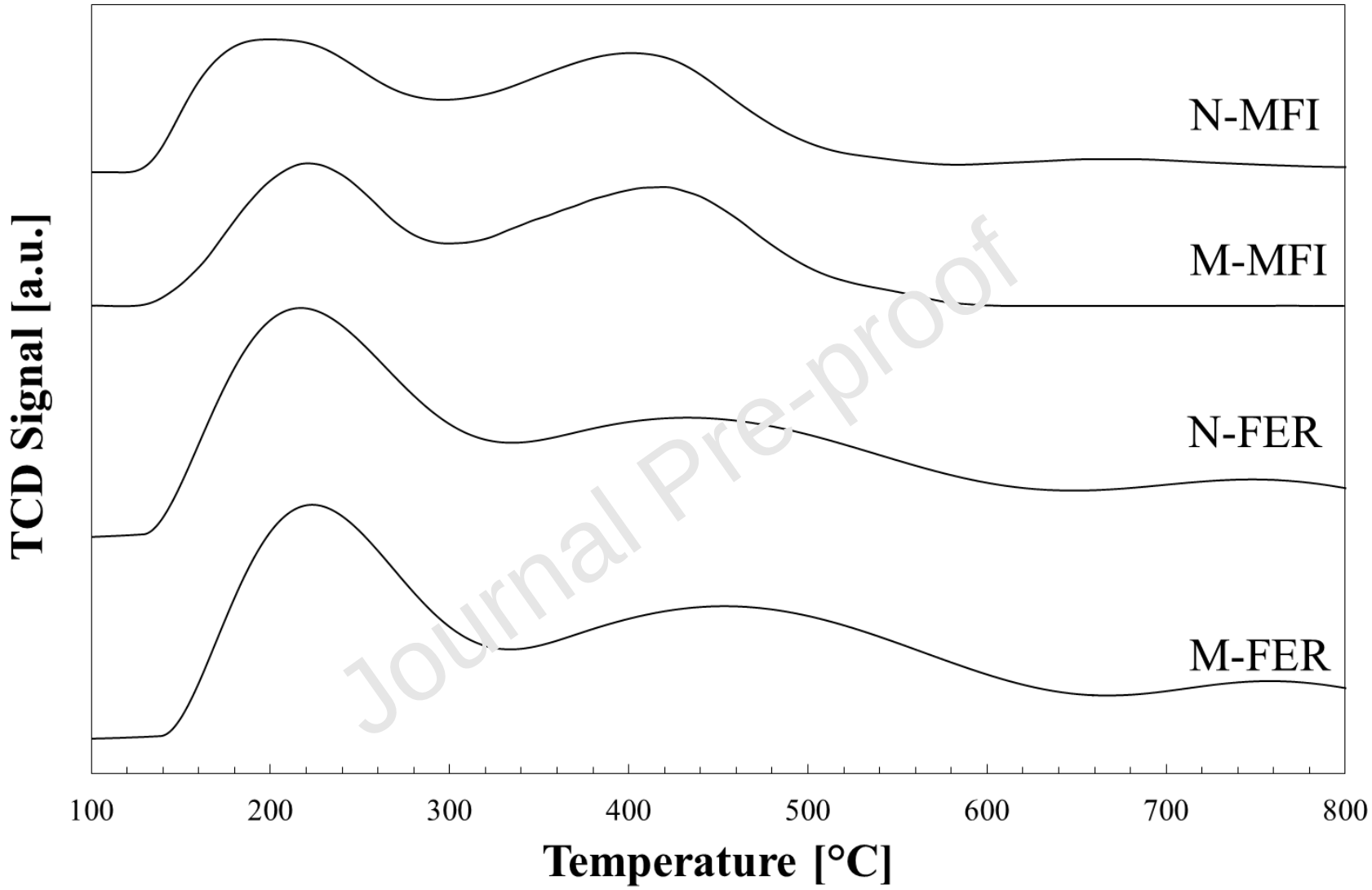

Figure 3

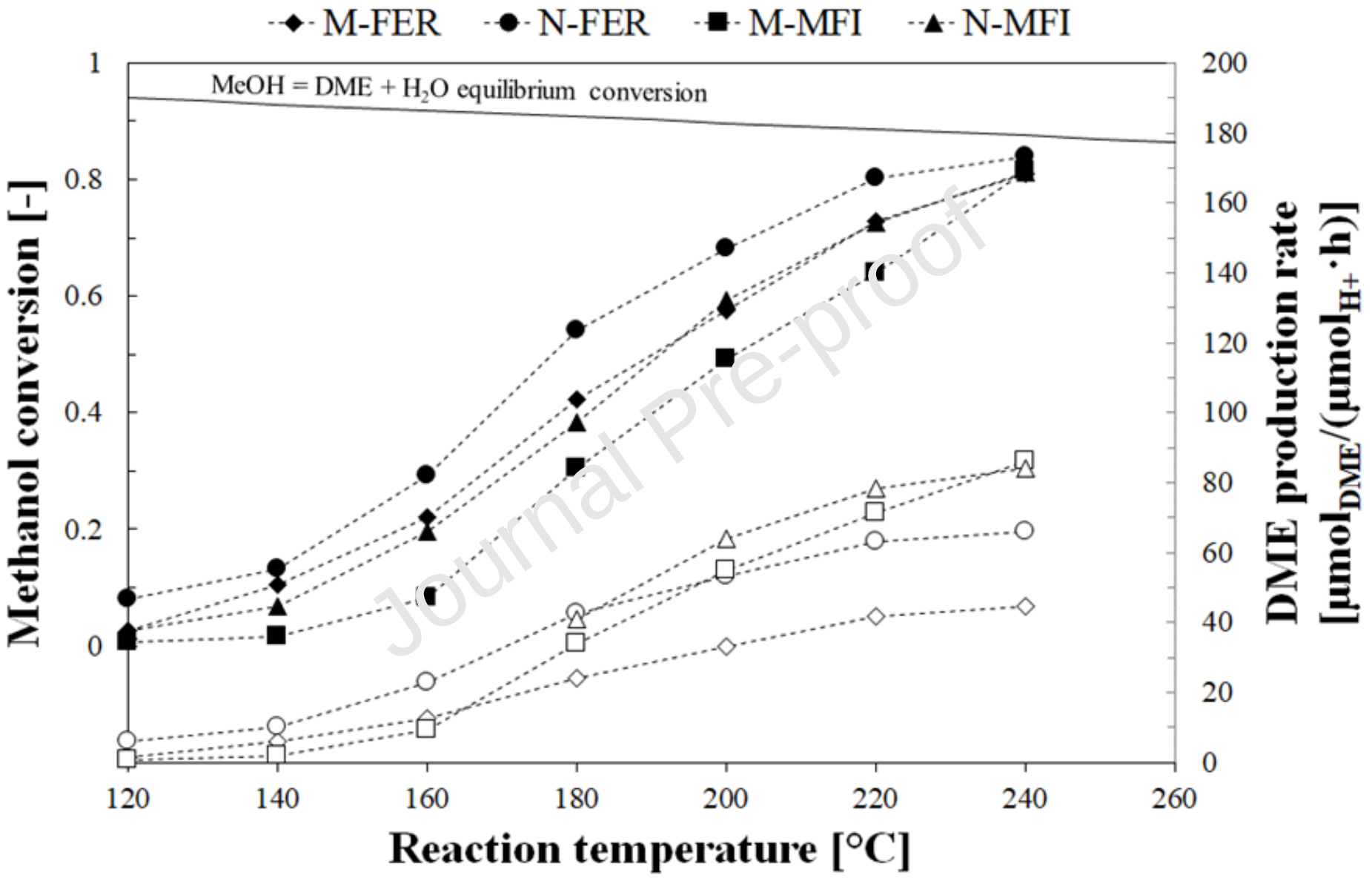

Figure 4

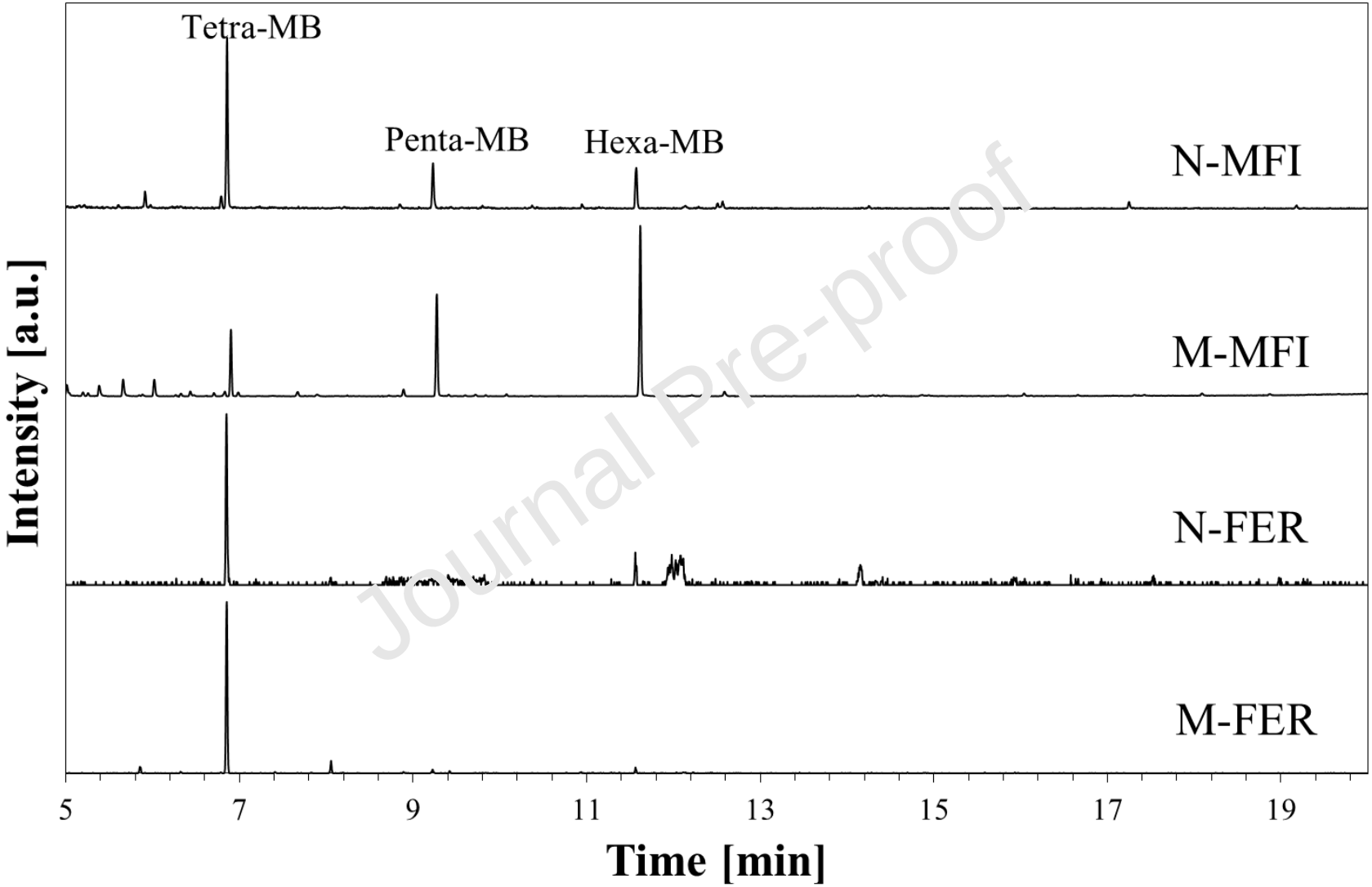

Figure 5

Figure 6

Highlights

- MFI- and FER-zeolites with different crystal size were synthesised.
- The effect of crystal size on methanol-to-DME reaction was studied.
- The reduction of crystal size improves DME production rate.
- The reduction of crystal size delays coke formation.
- Nano-sized MFI shows promising catalytic performances.

Figure 7